2018

Fruit Structure in Arabidopsis Thaliana Organ Boundary Mutants

Katelyn Childers
University of Mississippi. Sally McDonnell Barksdale Honors College

Fruit Structure in *Arabidopsis thaliana* Organ Boundary Mutants

By: Katelyn Elizabeth Childers

A thesis submitted to the faculty of The University of Mississippi in partial fulfillment of the requirements of the Sally McDonnell Barksdale Honors College.

Oxford
May 2018

Approved by:

_____
Advisor: Dr. Sarah Liljegren

_____
Reader: Dr. Stephen Brewer

_____
Reader: Dr. Ryan Garrick

ACKNOWLEDGMENTS

I owe a huge thanks to Dr. Sarah Liljegren for giving me the opportunity to join her lab. It is with her guidance and mentorship that I have been able to acquire a wealth a knowledge and experience. I am extremely proud of this thesis and none of it would have been possible without your help, critiques, and numerous hours of instruction.

I would also like to thank my family and friends to the continuous support throughout not only this research project, but my entire college career. The encouragement and kind words have kept me going even when times were tough. I owe all my successes to my amazing support system.

Thank you to Emily Fountain, Adam Harris, and Greta Parker for training me in the lab and assisting me in the completion of this research project. I owe thanks to Hayden Malone, Sam Palmer, Jack Mason, Luke Leary, and Hunter Roth for providing an enjoyable work environment and lending a helping hand when needed.

Last but not least, I would like to thank the Sally McDonnell Barksdale Honors College for the opportunity to complete this thesis. Though it was a daunting task at first, this has truly become an invaluable experience.

This research was supported by an NSF grant (IOS- 1453733) to SL.

ABSTRACT

KATELYN ELIZABETH CHILDERS: Fruit Structure in *Arabidopsis thaliana* Organ Boundary Mutants
(Under the direction of Dr. Sarah Liljegren)

The fruit are an integral plant organ that function to nurture and disperse seeds. Using the model species *Arabidopsis thaliana*, the genetic mechanisms underlying fruit development have been carefully studied. The *Arabidopsis* fruit originates from the female reproductive organ, the gynoecium, which consists of two carpels that develop into the ovary with a style and stigma. Proper formation of the fruit relies on a functional floral meristem and on the specification of boundary regions that arise between the carpel walls and a medial replum. Two genes known to affect both the development of organ boundaries in the flower as well as meristem maintenance are *SHOOT MERISTEMLESS (STM)* and the *ARABIDOPSIS THALIANA HOMEOBOX GENE1 (ATH1)*. *STM* and *ATH1* encode transcription factors from the homeodomain family. Combined mutations in the *STM* and *ATH1* genes blur the boundaries formed between the floral organs and the underlying stem.

To explore the functions of *STM* and *ATH1* during fruit development, I analyzed the size and structure of *stm*, *ath1*, and *stm ath1* mutant fruit compared to wildtype. Since *STM* is essential for maintenance of the stem cell population in shoot meristems, I expected that the size of *stm* single and *stm ath1* double mutant fruit would be reduced. If the *STM* and *ATH1* genes also have redundant roles in boundary formation in the fruit, I expected to see possible alterations in the structure of double mutant fruit. To quantify fruit growth defects of the single and double mutants compared to wildtype fruit, I measured the length and width of fruit, and determined the number of carpels present. I

found that the majority of *stm ath1* flowers did not produce a fruit and that the size of the *stm ath1* double mutant fruit present was severely reduced. Furthermore, the double mutant flowers exhibited a diverse array of unusual carpel-derived structures, some of which may be related to defects in boundary formation. My results indicate that the *STM* and *ATH1* genes have redundant functions during fruit development.

TABLE OF CONTENTS

ACKNOWLEDGMENTS iii

ABSTRACT iv

LIST OF FIGURES AND TABLES vii

LIST OF ABBREVIATIONS viii

INTRODUCTION 1

METHODS 11

I. Planting and Growth Conditions 11

II. Genotyping 12

III. Imaging 16

IV. Fruit Data Collection 16

V. Fruit Measurements 18

VI. Data Analysis 19

RESULTS 20

DISCUSSION 27

BIBLIOGRAPHY 30

LIST OF FIGURES AND TABLES

Table 1 Seed stocks used for experimentation

Table 2 Primers used for PCR amplification of DNA

Table 3 PCR conditions for amplification of genomic DNA

Table 4 Sample collection from wildtype, *stm, ath1,* and *stm ath1* plants

Table 5 Average fruit length and standard deviation for wildtype, *stm, ath1, and stm ath1* plants

Table 6 Average fruit width and standard deviations for wildtype, *stm, ath1,* and *stm ath1* plants

Figure 1 Fruit development of Wildtype *Arabidopsis thaliana*.

Figure 2 Diagram of floral organs in wildtype *Arabidopsis thaliana* flower

Figure 3 Ectopic expression of *FRUITFUL* prevents formation of the valve/replum boundary

Figure 4 Fruit of wildtype and *shp1 shp2* plant

Figure 5 Relationship of FUL, *SHP*, and RPL

Figure 6 Mutations in *STM* and *ATH1* homeodomain regions

Figure 7 Fruit pictures for fruit size measurements

Figure 8 Irregular fruit structures in *stm ath1-5* double mutant fruit

Figure 9 Average fruit length of wildtype, *stm, ath1,* and *stm/ath1* plants

Figure 10 Average fruit width of wildtype, *stm, ath1,* and *stm ath1* plants

Figure 11 Observed carpel number of 132 *stm/ath1* mutant samples

Figure 12 Average fruit length by plant

Figure 13 Percentage of Normal Carpel Development in wildtype, *stm,* and *ath1* plants

LIST OF ABBREVIATIONS

Arabidopsis: Arabidopsis thaliana

ALC: ALCATRAZ

ATH1: *ARABIDOPSIS THALIANA HOMEOBOX GENE 1*

ath1: ATH1 mutant

bHLH: basic helix-loop-helix

bp: base pair

ChIP-Seq: Chromatin immunoprecipitation sequencing

ddH_2O: deionized water

DNA: deoxyribonucleic acid

DZ: dehiscence zone

FM: floral meristem

FUL: FRUITFULL

ful: FRUITFULL mutant

IND: INDEHISCENT

KNOX: KNOTTED1-like homeobox

Ler: Landsberg *erecta*

mRNA: messenger RNA

PCR: polymerase chain reaction

RPL: *REPLUMLESS*

rpl: REPLUMLESS mutant

SAM: shoot apical meristem

SEM: scanning electron micrograph

SHP1: *SHATTERPROOF1*

shp1: SHATTERPROOF1 mutant

SHP2: *SHATTERPROOF2*

shp2: SHATTERPROOF2 mutant

STM: *SHOOT MERISTEMLESS*

stm: STM mutant

T-DNA: transfer DNA

WT: wildtype

INTRODUCTION

Many flowering plants follow evolutionarily conserved pathways in the development of their floral organs. The fruit arises from the gynoecium—the highly specialized female reproductive structure of a plant that allows for maturation and dispersal of seeds (Ferrándiz et al., 2000). *Arabidopdis thaliana,* a model organism for plant genetics, produces fruit composed of a stigma, style, and two fused carpels. Following fertilization, the pistil undergoes a rapid increase in growth and gives rise to the fruit, which is comprised of multiple cell types (Ripoll et al., 2011). The carpel walls, known as valves, connect to the replum, which forms a middle ridge that defines the margin of the two carpels (Liljegren et al., 2004; Figure 1). The fruit, known as a silique, splits open or dehisces to release its seeds upon maturity. Its development is marked by extensive cell division and elongation in response to signals from the rapidly growing seeds (Müller, 1961; Alonso-Cantabrana et al., 2007).

Figure 1 illustrates the structure of a wild-type fruit and the cell types that contribute to fruit opening. Cells at the replum/valve boundary differentiate into the dehiscence zone (DZ), or separation layer (Figure 1). Dehiscence is the process of detachment of the valves from the replum after seed maturation, thereby allowing for seed dispersal. Cells at the valve margin adjacent to the separation layer exhibit lignification, and lignification also occurs in the valve's inner subepidermal layer (Figure 1). This reinforcement of specific cell types is thought to contribute to fruit opening by providing tension within the valve (Ripoll et al., 2011).

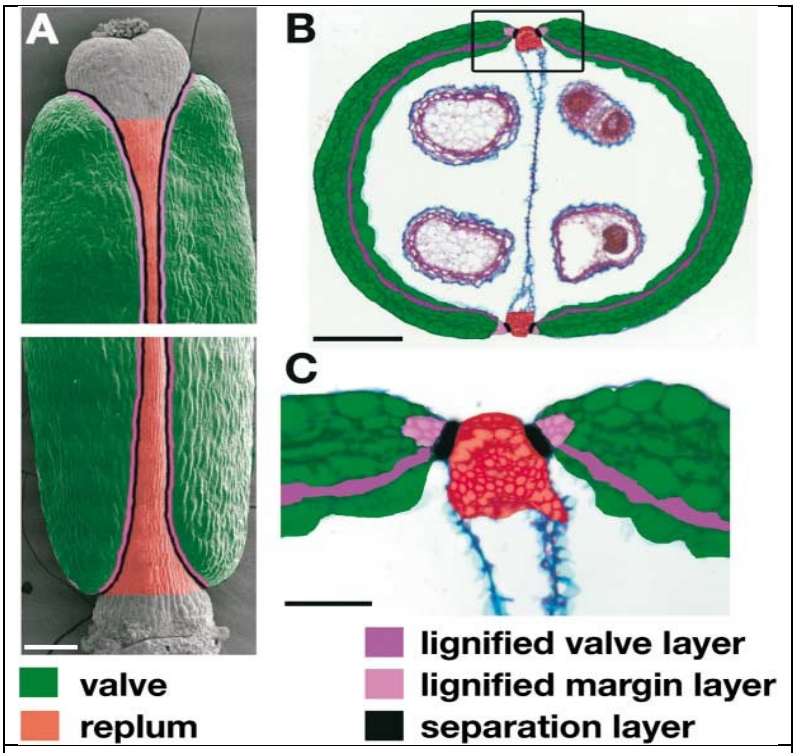

Figure 1: Fruit development in *Arabidopsis thaliana*. A) Scanning electron micrographs of mature wildtype fruit. The fruit regions are colorized. B) Transverse section of wildtype fruit showing distinct cell types. C) Magnified view of valve margin region. (Photo credit: Liljegren et al., 2004)

Arabidopsis is a useful model organism due to its short lifespan, easily replicated growth conditions, and small and extensively studied diploid genome that consists of five chromosomes (Meinke et al., 1998). Another advantage of *Arabidopsis* is that its flowers normally undergo self-pollination, which allows for the genotypes of offspring to be controlled. Figure 2 displays a diagram of a wildtype *Arabidopsis* flower. The number and position of the floral organs are constant among wildtype plants, with four concentric rings of organs—four sepals, four petals, six stamens, and two fused carpels forming the gynoecium (Dinneny et al., 2005). Genetic studies have revealed the function of several key genes required for fruit development.

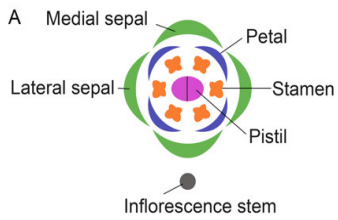

Figure 2: Diagram of a wildtype *Arabidopsis* flower. Four sepals surround four petals which encircle six stamens. The pistil includes two fused carpels that make up the gynoecium. (Image credit: Gubert et al., 2014)

FRUITFULL (FUL) is a MADS-box gene essential for development of the valve cells and fruit growth. A study by Gu et al. (1998) found that, post-fertilization, the *ful* mutation blocks elongation of the silique, thereby producing an underdeveloped organ that is overwhelmed with seeds; hence, the gene was named *FRUITFULL*. In transgenic plants that constitutively express *FUL* throughout the gynoecium, cells at the valve/replum margin are converted into valve cells and valve margin lignification does not take place (Ferrándiz et al., 2000). This erasure of the valve/replum boundary in gain-of-function *35S::FUL* fruit prevents normal DZ development and seed dispersal (Figure 3).

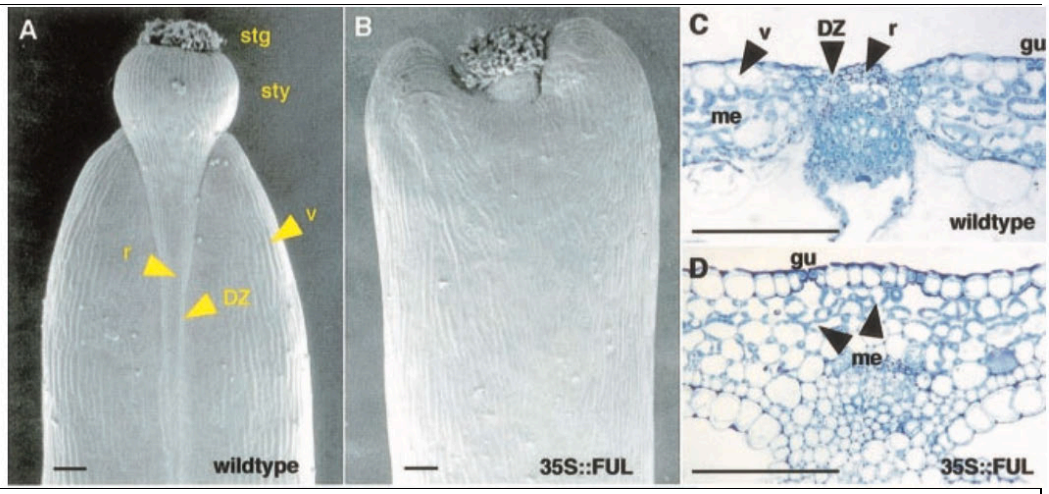

Figure 3: Ectopic expression of *FRUITFUL* prevents formation of the valve/replum boundary. A) SEM of wildtype fruit with normal apical stigma, style, replum, valve, and dehiscence zone development. B) SEM of gain of function *35S::FUL* fruit that fails to form a dehiscence zone. C) Transverse section through a wildtype fruit with normal dehiscence zone development and valve margin lignification. D) Cells at the valve/replum boundary of *35S::FUL* fruit take on a similar fate as wildtype valve cells due to ectopic FUL activity. (Photo credit: Ferrándiz et al., 2000).

Two other closely related MADS-box genes, *SHATTERPROOF1 (SHP1)* and *SHATTERPROOF 2 (SHP2),* regulate formation of the separation layer and promote lignification of the adjacent valve margin cells (Liljegren et al., 2000). *SHP1* and *SHP2* are expressed at the valve/replum boundary and function redundantly; mutations in either gene alone do not disrupt fruit development, while mutations in both genes prevent fruit dehiscence (Figure 4). *shp1 shp2* double mutant fruit fail to open, leaving the seeds trapped inside. In *ful* mutant fruit, *SHP1* and *SHP2* expression expands into the valves, suggesting that FUL acts to restrict *SHP1* and *SHP2* expression (Ferrándiz et al., 2000; Figure 5). The SHP1 and SHP2 transcription factors control valve margin identity by activating two downstream genes, *INDEHISCENT (IND)* and *ALCATRAZ (ALC),* that encode basic helix-loop-helix (bHLH) transcription factors (Liljegren et al., 2004). IND,

ALC, SHP1 and SHP2 work together as a regulatory network to coordinate differentiation of the valve/replum boundary, allowing for the process of fruit dehiscence. Mutations in *IND*, *ALC*, *SHP1* and *SHP2* were found to suppress the growth defects of *ful* fruit (Liljegren et al., 2004). These results suggest that rather than promoting fruit expansion, the key function of the FUL transcription factor in the valves is to set a boundary for expression of the genes responsible for valve margin differentiation (Figure 5). Negative regulation of *IND*, *ALC*, *SHP1* and *SHP2* by FUL assures that valve margin differentiation ensues only at the edge of the valve, and prevents the valves from assuming a valve margin cell fate (Roeder et al., 2003).

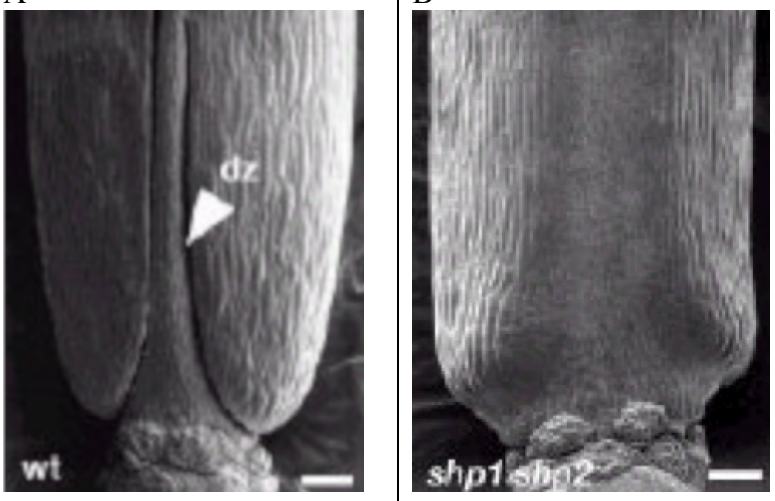

Figure 4: *Arabidopsis* fruit of wildtype and *shp1 shp2* plants. A) SEM of wildtype fruit with normal valve margins and dehiscence zone. B) *shp1 shp2* double mutant fruit with defective valve margin. (Photo credit: Liljegren et al., 2000)

In a study by Roeder et al. (2003), *REPLUMLESS (RPL)* was identified as a requirement for replum development; this gene encodes a homeodomain transcription

factor that prevents replum cells from adopting a valve margin cell fate by negative regulation of *SHP1 and SHP2* expression. Genes that belong to the homeodomain family of TFs have a conserved DNA binding domain termed the homeodomain. It was discovered that *rpl* fruit are missing a medial replum and in its place have narrow cells that are similar to valve margin cells. However, replum development was found to be rescued in *rpl shp1 shp2* triple mutant fruit. This result suggests that RPL is not a direct necessity for replum formation; rather, RPL is essential to prevent the expression of *SHP1* and *SHP2* in replum cells, thereby stopping these cells from assuming valve margin cell fate. With their respective activities in the replum and the valve, RPL and FUL restrict expression of *SHP* to a thin stripe at the valve/margin boundary (Figure 5).

Some interactions that occur in forming boundaries between the shoot apical meristem (SAM) and new leaf and flower primordia that arise on the flanks of the SAM are similar to the events involved in establishing the fruit valve/replum boundaries (Alonoso-Cantabrana et al., 2007). The fruit replum, which has meristematic properties, shows expression of *SHOOT MERISTEMLESS* (*STM),* a gene used in my study. STM is required for the formation of the carpel marginal meristem, which is a ridge of meristematic tissue that differentiates from the replum and eventually gives rise to the ovules (Hepworth and Pautot, 2015). Since STM and other class I KNOTTED-LIKE (KNOX) transcription factors are expressed in the replum, but not the valves, it is possible that STM is involved in activation of *RPL* (Girin et al., 2009) (Figure 5).

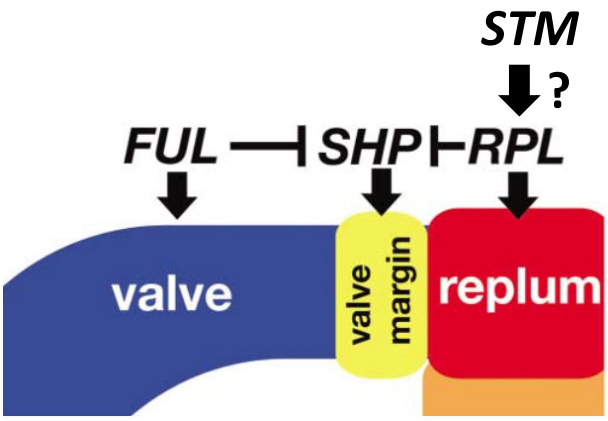

Figure 5: Relationship of FUL, *SHP*, RPL and STM. The STM homeodomain transcription factor activates *RPL*. The RPL homeodomain transcription factor restricts expression of the *SHP* MADS-box gene from the replum; The FUL MADS-domain transcription factor prevents expression of *SHP* in the valves. (Modified from Roeder et al., 2003)

The primary role of STM in plant development is to replenish stem cells in the shoot apical meristem (SAM) and floral meristem (FM) (Scofield et al., 2014). STM maintains the stem cell population at the center of the SAM by synthesizing cytokinin to promote cell division. STM also delays organ differentiation and inhibits growth in the peripheral region of the SAM to establish lateral organ boundaries with new leaf and flower primordia on its flanks (Jasinski et al., 2005; Yanai et al., 2005). Previous research has shown that loss-of-function mutations in *STM* result in the absence of a SAM altogether and fusion between cotyledons of seedlings (Long et al., 1996). A novel *stm* mutant is the result of a point mutation that changes tryptophan (W) to a premature stop codon at amino acid 343 (Figure 6; Liljegren, unpublished results). This mutation

occurs in the homeodomain region of the STM transcription factor but only partially knocks out STM function.

ARABIDOPSIS THALIANA HOMEOBOX GENE1 (*ATH1*) encodes a BELL-type homeodomain transcription factor (Quaedvlieg et al., 1995). Previous studies have shown that the *ATH* and *STM* genes are both involved in the formation of the organ boundary regions between floral organs and stems of *Arabidopsis* flowers (Gómez-Mena and Sablowski, 2008, Liljegren, unpublished results). ATH1 restricts growth in cells at the junction between the stem and floral organs. A novel *ath1* allele has a splice site error that is predicted to introduce a premature stop codon at the tyrosine (Y) amino acid at position 399; this mutation occurs in the DNA-binding region of the protein (Figure 6; Liljegren, unpublished results). The phenotype of this mutant closely resembles that of a previously reported *ath1* loss-of-function mutant (Gómez-Mena and Sablowski, 2008).

Analysis of flowers from the single *ath1* mutant and weak *stm* mutant revealed that these mutations reduce the definition of the lateral organ boundaries that form between the bases of floral organs and underlying stems. This results in fusion of the stamens at their bases and prevents their detachment after pollination (Palmer, 2018). In *ath1 stm* mutant flowers, the lateral organ boundary between the sepals and the floral stem is missing, and the outer organs fail to abscise (Liljegren, unpublished results; Palmer, 2018). Defects in forming boundaries between adjacent floral organs results in a substantial number of stamen-stamen and sepal-sepal fusions in *stm ath1* flowers (Malone, 2018; Leary, 2018).

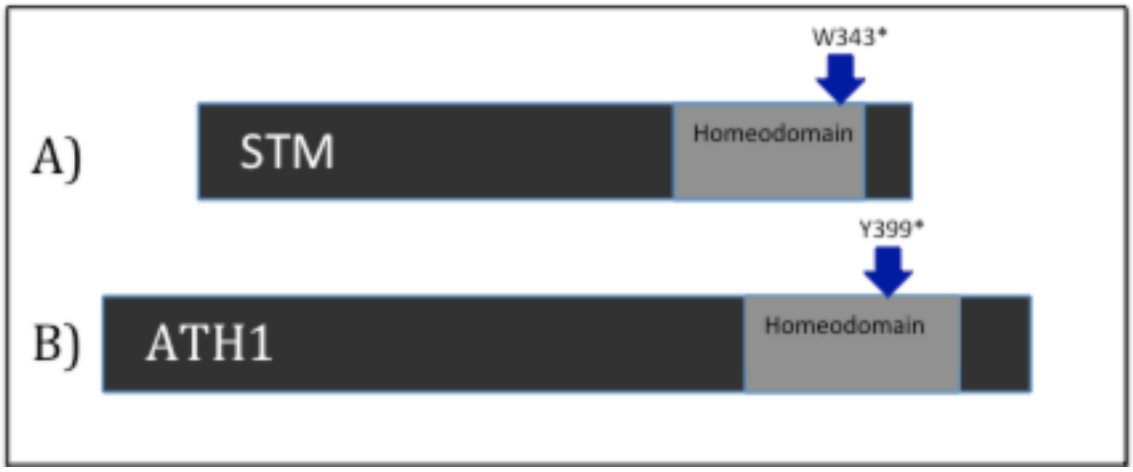

Figure 6: Mutations in *STM* and *ATH1* affect the homeodomain regions of the encoded transcription factors. A) The *stm* point mutation introduces a premature stop codon at position 343. **B)** A splice site error on the *ATH1* gene is predicted to introduce a stop codon at position 399. The W and Y represent the tryptophan and tyrosine amino acids, respectively. (Image credit: Liljegren, unpublished results)

Although STM functions to regulate gene transcription in the nucleus, it does not have a nuclear localization signal in its amino acid sequence (Cole et al., 2006). Because it lacks this signal, STM cannot enter the nucleus on its own. ATH1 has a nuclear localization signal in its amino acid sequence and is found in both the cytoplasm and the nucleus (Rutjens et al., 2009). STM has been found to heterodimerize with ATH1 as well as other BELL-type homeodomain transcription factors. This allows for ATH1 and other interacting partners to bring STM into the nucleus in order for transcription to occur. *ath1* single mutants have slight phenotypic defects in the SAM because STM heterodimerizes with ATH1 and two other BELL-type transcription factors in that developmental context

(Rutjens et al., 2009). Genetic studies have shown that plants containing mutations in *ATH1*, *REPLUMLESS* (also called *PENNYWISE*) and *POUNDFOOLISH* mimic *stm* loss-of-function mutants and prevent formation and maintenance of the SAM (Rutjens et al., 2009).

The goal of this study was to investigate the phenotypic defects of *stm* and *ath1* mutations on fruit development. A previous study of floral organ count in *stm ath1-5* flowers noted missing fruit and unusual structures (Malone, 2018); the idea for this project came in part from this unexpected discovery. My first hypothesis was that fruit size would be reduced in the *stm ath1* double mutant due to ATH1 and STM's role in flower meristem maintenance. A second, related hypothesis was that the number of carpels in *stm ath1* fruit would be less than the two typically found in wildtype fruit. Changes in carpel number have been previously reported for other mutations that alter the size of the flower meristem (Penin and Logacheva, 2011). Another contributing factor to a change in carpel number in *stm ath1* fruit may due to disruption of fruit boundary patterning and loss of the medial replum region (Girin et al., 2009). I will investigate these defects by measuring fruit length and width and examining the number of carpels of wildtype, *stm* single mutant, *ath1-5* single mutant, and *stm ath1-5* double mutant genotypes.

METHODS

I. Planting and Growth Conditions

Arabidopsis seeds need a cold treatment to simulate winter before they can germinate. The seeds were sterilized before planting by covering with 70% ethanol for two minutes. Once the ethanol was removed, the seeds were soaked with a 5% bleach 1% SDS solution and allowed to sit for 15 minutes. The bleach solution was removed and 500μL of distilled and deionized water (ddH_2O) was added and removed three times. After adding another 500μL of ddH_2O, the seeds were left in a 4°C refrigerator for two days. Before planting, the ddH_20 was removed and the seeds were suspended in a 0.1% agarose solution.

The wild-type plants used for this experiment were of the Landsberg *erecta* (Ler) ecotype. The seeds planted for the mutant genotypes were *stm*, *ath1-5*, and *stm ath1-5/+* (Table 1). Plants with homozygous mutations in both the *STM* and *ATH1* genes are infertile, so a seed stock collected from a plant which is homozygous for one mutation and heterozygous for the other mutation was used. Since these genes are not linked, it was expected that 25% of the seeds should have the *stm ath1* genotype. Three trays of ten pots were planted of the *stm/ath1-5+* seed stock. One tray consisting of ten pots was planted for the other genotypes.

The plants were potted in damp Promix BX soil. The pots were labeled with the respective genotype for organization. A 200μL pipette was used to plant nine seeds per pot. A lid was placed on each tray in order to provide a humid environment for the seedlings. After about a week, the sprouts were picked through to avoid root tangling, Marathon 1% granular pesticide was added, and the lid was removed. The plants were

watered Monday, Wednesday, and Friday alternating between water and Miracle Grow (200ppm). Growth conditions were 16 hours of light and eight hours of dark at a controlled temperature of 23°C and 70% humidity. This process was carried out with the help of Emily Fountain.

Table 1: Seed Stocks Used for Experimentation

Seed Stock Name	Number of Trays Planted	Date of Seed Collection	Possible Genotypes
"LER WT B"	1	11/16/2018	WT
"sta1 #1"	1	5/25/2017	*Stm*
"sta2 #7"	1	6/5/2017	*ath1-5*
"sta1/+ sta2 #178 #2"	1	11/16/2017	*stm ath1-5, stm/+ ath1-5, STM ath1-5*
"sta1/+ sta 2 #178 #7"	1	11/15/2017	*stm ath1-5, stm/+ ath1-5, STM ath1-5*
"sta 1/+ sta 2 #21-#25"	1	1/5/2017	*stm ath1-5, stm/+ ath1-5, STM ath1-5*
"sta1/+ sta2 #1"	1	11/15/2017	*stm ath1-5, stm/+ ath1-5, STM ath1-5*
"sta1/+ sta2 #38?	1	10/16/2017	*stm ath1-5, stm/+ ath1-5, STM ath1-5*

II. Genotyping

DNA Extraction:

Genomic DNA was prepared using leaves of mutant plants and the Plant DNeasy© Plant Mini Kit (QIAGEN©). Tissue samples were disrupted using a tissue pulverizer. 400μL of lysis buffer (Buffer AP1) for lipid disruption and 4μL of RNase A for RNA breakdown were added to the tissue samples, then each sample was vortexed and incubated for ten minutes at 65°C. 130μL of precipitation buffer (Buffer P3) for neutralization was then added, mixed, and incubated for five minutes on ice. Following incubation, the lysate was centrifuged for five minutes at 14000 rpm. The lysate was pipetted into a QlAshredder spin column placed in a 2 mL collection tube. The lysate was

centrifuged for two minutes at 14000 rpm. Flow-through was transferred into a new tube without disturbing the pellet. 1.5 volumes of binding buffer (Buffer AW1) for protein denaturing was added and mixed by pipetting. 650µL of the mixture was transferred into a DNeasy© Mini spin column placed in a 2mL collection tube. The mixture was centrifuged for one minute at 8000 rpm. Flow-through was removed and discarded, and the process repeated with the remaining sample. The spin column was placed in a new 2mL collection tube and 500µL of Buffer AW2 for salt removal and purification was added. The mixture was centrifuged for one minute at 8000 rpm and flow-through discarded. Another 500µL of Buffer AW2 was added and the mixture was centrifuged for two minutes at 14000 rpm. The spin column was transferred to a new 2mL microcentrifuge tube. 100µL of a low-salt buffer (Buffer AE) was added for elution and incubated for five minutes at room temperature and then centrifuged for one minute at 8000 rpm. The step was repeated. The plant genomic DNA was stored at -20°C.

Polymerase Chain Reaction:

In order to genotype the mutant plants, Polymerase Chain Reaction (PCR) was used to amplify the *STM* and *ATH1* gene regions using mutant genomic DNA as a template. A master mixture was created using a per reaction ratio of 2µL of 10X Standard Taq Reaction Buffer, 0.5µL of 10mM dNTP, 0.7µL of 20 mM forward and reverse primers, 0.5µL of Taq DNA Polymerase, and 13µL ddH_2O. 20µL PCR mixtures were made with 18µL of the master mixture and 2µL of genomic DNA. The samples ran on either a *STM* PCR cycle or an *ATH1* PCR cycle in an S1000 Thermal Cycler. The primer

sequences can be seen in Table 2. The conditions of the PCR were optimized for each set of primers and can be viewed in Table 3.

Table 2: Primers used for PCR amplification of targeted gene regions

Primer Name	Sequence (5'-3')
ATH1 Forward	GGATGTTCCAAAACTTCCTTCACCC
ATH1 Reverse	GCTTGATTTTTTCCTAGCCCTAATCTC
STM Forward	GTTCATAAACCAGAGGAAACGGCACTG
STM Reverse	GAGGAGATGTGATCCATTGGGAAAGG

Table 3: PCR conditions for amplification of targeted gene regions

	STM		*ATH1*	
Step	Temperature (°C)	Time (seconds)	Temperature (°C)	Time (seconds)
1	94	240	94	240
2	94	30	94	30
3	55	30	54	30
4	72	30	72	30
5	Repeat steps 2-4 30 times	Repeat steps 2-4 30 times	Repeat steps 2-4 30 times	Repeat steps 2-4 30 times
6	4	Forever	4	Forever

Ethanol Precipitation:

Due to the high concentration of salt in the PCR buffer, which can disrupt activity of some restriction enzymes, the *ATH1* PCR products were desalted via ethanol precipitation. After completion of PCR, 60μL of 100% ethanol (stored at -20°C) and 2.1μL of 3M sodium acetate at pH 5.2 was added. The sample sat overnight at -20°C. The samples were centrifuged at 4°C and 15000 rpm for 45 minutes. The ethanol supernatant was removed leaving the pellet undisturbed. After, 250μL of 70% ethanol (stored at -20°C) was added. The sample was spun down at 4°C and 15000 rpm for 15

minutes. Ethanol was removed leaving the pellet undisturbed, and the sample was put in a 37°C water bath to evaporate any remaining ethanol without drying out the pellet. Following evaporation, the pellet was resuspended in 20μL ddH_2O and used for restriction enzyme digest reactions.

Restriction Enzyme Digest:

Homozygous *stm* mutant plants were distinguished from wildtype and heterozygous plants based on a BsrI restriction site present in only the wild-type allele of the *STM* PCR product. Using BsrI to digest the PCR products allows the genotype of the samples to be viewed after separating digested PCR products by size using gel electrophoresis. The reaction ratio for this digest is 17uL of the PCR product, 2uL of 10X NEBuffer 3.1, and 1uL of BsrI (New England BioLabs). Each 20uL sample was then incubated at 65°C for four hours. The wildtype PCR product was cut into 106 bp and 29 bp fragments, whereas the uncut *stm* mutant PCR product was 135 bp.

Homozygous *ath1* mutant plants were distinguished from wildtype and heterozygous plants based on a MIuCI restriction site present in only the wild-type allele of the *ATH1* PCR product. *ATH1* PCR products were digested using a MluCI (New England BioLabs) restriction enzyme in the recommended enzyme buffer, CutSmart™ Buffer (New England BioLabs). The mutant PCR product was cut into 306 bp, 158 bp, and 115 bp fragments. Samples (3uL master mix, 17 uL PCR) were incubated at 37°C for three hours.

Gel Electrophoresis:

Digested DNA samples were analyzed using gel electrophoresis, which separates the sample by the length of the DNA fragments. Powdered agarose was melted in 1X TAE buffer and ethidium bromide was added to the solution. The liquid was poured in a gel mold with a comb to create the wells and allowed to sit at room temperature to solidify. Due to the small difference in size of *STM* PCR products, a 3% agarose gel was used to separate the fragments (made with 6g agarose, 200mL TAE, and 5.5μL ethidium bromide). A 1% agarose gel was used for observing *ATH1* PCR products (made with 2g agarose, 200mL TAE, and 5.5μL ethidium bromide). 3μL of loading dye was added to each digest sample, then 13μL of each *ATH1* digest sample was loaded onto 1% agarose gel and 13μL of each *STM* were loaded onto the 3% gel. Gels were ran at 100V.

III. Imaging

Gel images were taken with an AlphaImager HP. The DNA was visible under ultraviolet light due to its interaction with ethidium bromide during gel electrophoresis. A 50bp ladder was used for the 3% gel and a 1000bp ladder was used for the 1% gel; these help to identify the base pair sizes of DNA fragments.

Images of fruit were taken from an Apple iPhone Model 7s. An NIH ImageJ program was used for measuring data from individual fruit as described below.

IV. Fruit Data Collection

Fruit from 10 wildtype plants were collected and imaged first. Five stage 17 fruit from the primary inflorescence of each plant were analyzed, beginning with the oldest fruit at stage 17 of flower development (Smyth, 1990) and fruit at the next four positions

moving up the primary stem. The fruit were observed under a dissecting microscope to identify the number of carpels. After carpel number was determined, the fruit were placed on a sheet of paper (in order of position) next to a millimeter ruler, and overhead pictures of the fruit were taken for later use (see Figure 7). This was done for all 10 wildtype plants. The average position of the oldest stage 17 fruit in the wildtype plants was calculated to use as a guide for selecting the corresponding age range of the mutant fruit analyzed. This position, five (corresponding to the fifth flower produced by the plant), was then used for the mutant genotypes: *stm, ath1,* and *stm ath1*. Ten *stm* and five *ath1* mutant plants were observed starting at the fifth position until the last fruit in stage 17. If the fifth position was already past stage 17, subsequent positions were checked until the first one at stage 17 was found. Carpel number was assessed, then a picture of the fruit (in ascending order of position) was taken.

Eight *stm ath1* double mutant plants were also observed starting at the fifth position (or subsequent first position at stage 17) until the last stage 17 flower. A piece of double-sided tape was placed on a microscope slide. The fruit were placed, in order of position, on the tape. This modification was used since the floral organs of the double mutant plants do not abscise, and allowed for repositioning the fruit or removal of other floral organs to get a better view of the carpels. The number of carpels were recorded and a picture of the fruit was taken after placement next to a ruler.

A

B

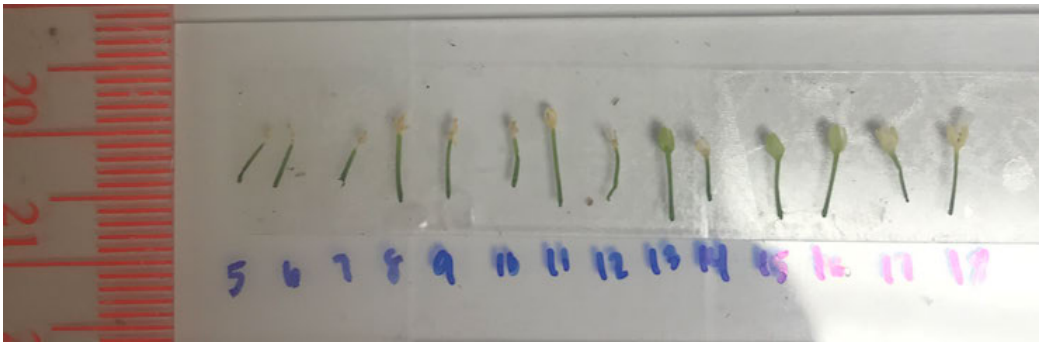

Figure 7: Fruit pictures for fruit size measurements. The fruit were lined up in order of ascending position number and placed next to a millimeter ruler for measurement calibration. A) Fruit of one wildtype plant with fully abscised floral organs and average fruit size. B) Fruit of an *stm ath1-5* double mutant plant with floral organ retention and defective fruit size.

V. Fruit Measurements

Images were uploaded to the NIH ImageJ computer program. The magnification of each image was calibrated using a ruler photographed with the fruit. Using the software to zoom in on each fruit, the length of each fruit was analyzed, as well as the width at its widest part. This was done for all of the fruit of each genotype.

VI. Data Analysis

Microsoft Excel was used to perform data analysis and generate bar graphs and pie charts. Average fruit length per plant was calculated by adding the lengths of each fruit for the respective plant and dividing by that plant's number of fruit. This was done for each plant in each genotype. The average of each genotype was calculated by dividing by the number of fruit analyzed for that genotype. This process was also done to calculate average fruit width. To assess the possibility that individual plants within a genotype could be outliers, the average for each plant within a genotype was calculated. Both the standard deviation and standard error were calculated using Microsoft Excel. Statistical significance was interpreted by whether or not the standard error bars overlapped between different sample groups.

RESULTS

This experiment was designed to investigate the phenotypic effects of mutations in *STM* and *ATH1* either alone or together on fruit development—specifically on fruit size, carpel number, and definition of the valve/replum boundary. Once I confirmed the genotype of *stm, ath1,* and *stm ath1* plants using PCR and restriction enzyme digests, phenotypic data were collected from a set of fruit on the primary inflorescence of each plant. Data were collected from the fruit at floral development stage 17; wildtype flowers are elongated green seedpods that have abscised all of their outer floral organs (Smyth et al., 1990). Multiple flowers at stage 17 were examined from each plant, as summarized in Table 4. The number of carpels per fruit for each genotype were observed using a dissecting microscope and recorded.

Table 4: Sample collection from wildtype, *stm, ath1,* and *stm ath1* plants

Genotype	# Plants Sampled	# Flowers Sampled
WT	10	50
Stm	10	232
ath1	5	54
stm ath1	8	48

As shown in Figure 10, all wildtype fruit were composed of two carpel valves, and defined by a central replum. This was also true for each fruit analyzed from the *stm* and *ath1* single mutants (Figure 10). In contrast, the majority (65%) of *stm ath1* double flowers analyzed were missing a fruit (Figure 9). A diverse array of irregular structures were observed in *stm ath1* double flowers with fruit (Figures 8 and 9). While some of the *stm ath1* flowers produced fruit with two carpel valves (10%), most of the *stm ath1*

flowers with fruit were composed of one carpel valve (11%) or contained pistil-derived structures without discernable valve tissue (14%).

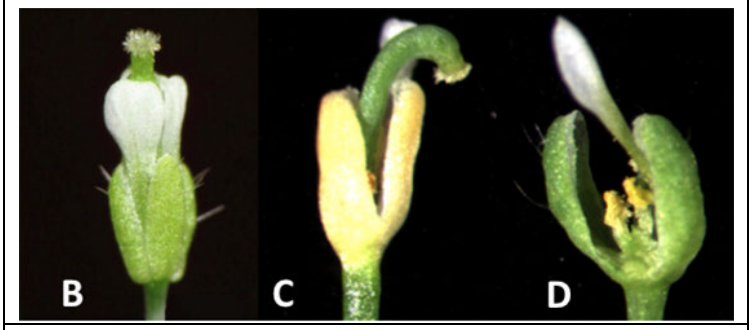

Figure 8: Irregular fruit structures in *stm ath1-5* double mutant fruit. A variety of fruit structures were seen when examining double mutant fruit. B) A relatively normal but smaller fruit. In my study, these fruit were found to have two carpels. C) A deformed fruit. In my study, fruit with this appearance were found to have one carpel only. D) A flower with the pistil missing completely (Photo credit: Hayden Malone)

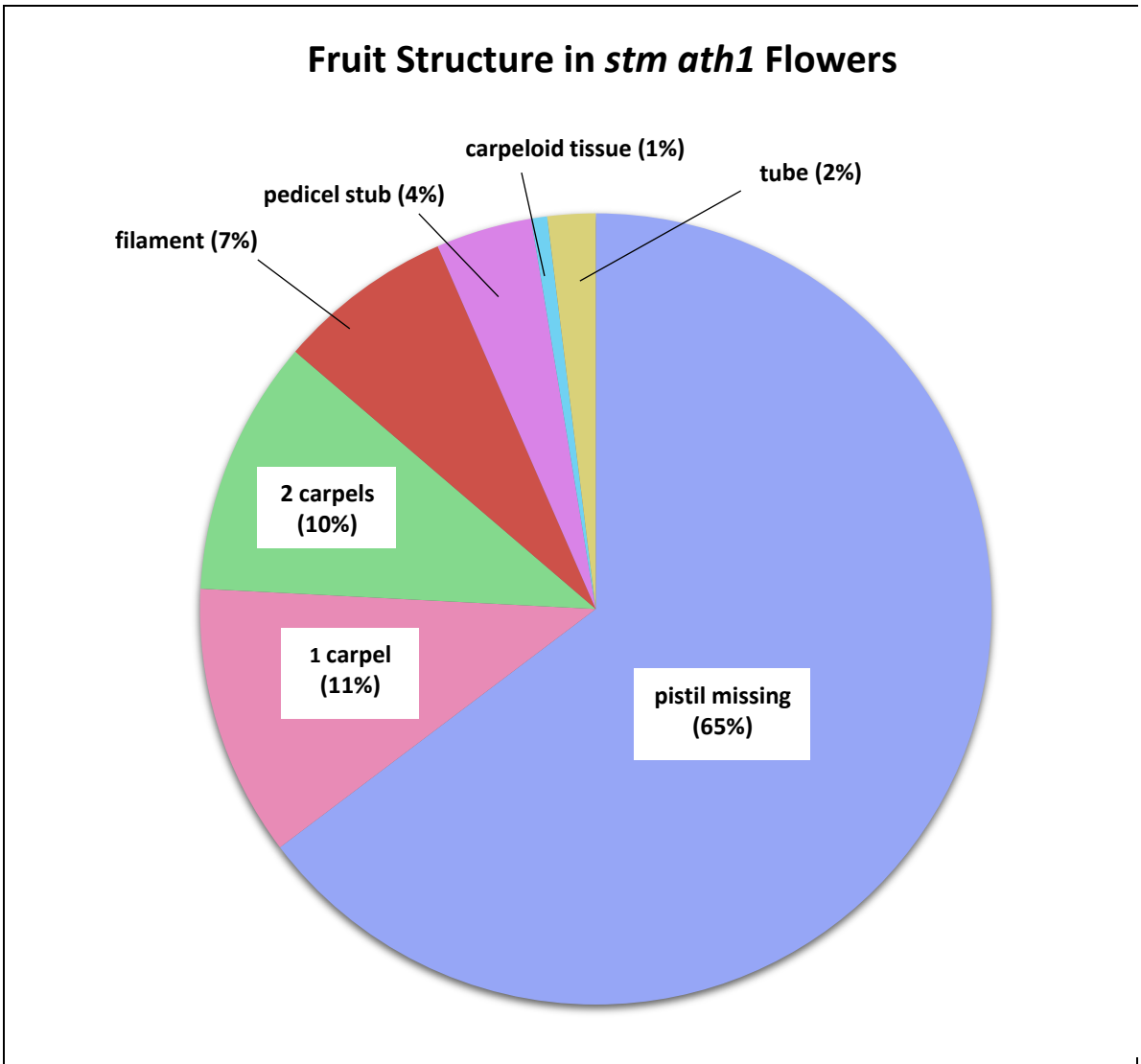

Figure 9: Fruit structure of *stm/ath1* mutants. Of the *stm ath1* double mutant flowers analyzed (n=132), 99 (65%) were missing a central pistil. 17 (11%) produced fruit with 1 carpel. 16 (10%) developed fruit with 2 carpels. 11 (7%) produced filaments. 6 (4%) produced pedicel stubs. 3 (2%) produced tubes, and 1 (1%) developed carpeloid tissue.

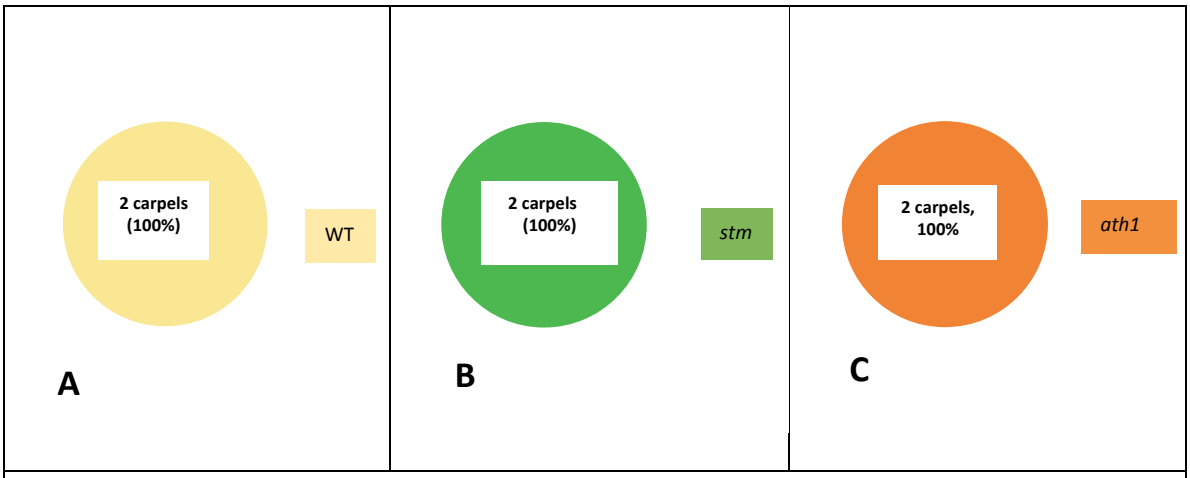

Figure 10: Fruit structure in wildtype, *stm,* and *ath1* plants. Each flower of every genotype analyzed produced a fruit with 2 carpels. A) n=50 for wildtype plants B) n= 232 for *stm* mutant plants. C) n=54 for *ath1* mutant plants.

Fruit produced by wild-type and mutant plants were imaged to analyze fruit size (see Figure 7). The NIH ImageJ program was used to calibrate the magnification of the photos and measure the length and width of each fruit. The average length of fruit for each genotype is shown in Table 5 and Figure 11. The average length of fruit for each plant within the genotypes analyzed is shown in Figure 12. Compared to wildtype, the *stm* single mutant, the *ath1* single mutant, and the *stm ath1* double mutant each show a significant reduction in fruit length.

Table 5: Average fruit length and standard deviation for wildtype, *stm, ath1, and stm ath1* plants

Genotype	Average Length (mm)	Standard deviation	Standard Error
WT	10.94	0.83	0.13
Stm	5.15	2.00	0.13
ath1	8.40	2.74	0.37
stm ath1	2.36	1.06	0.15

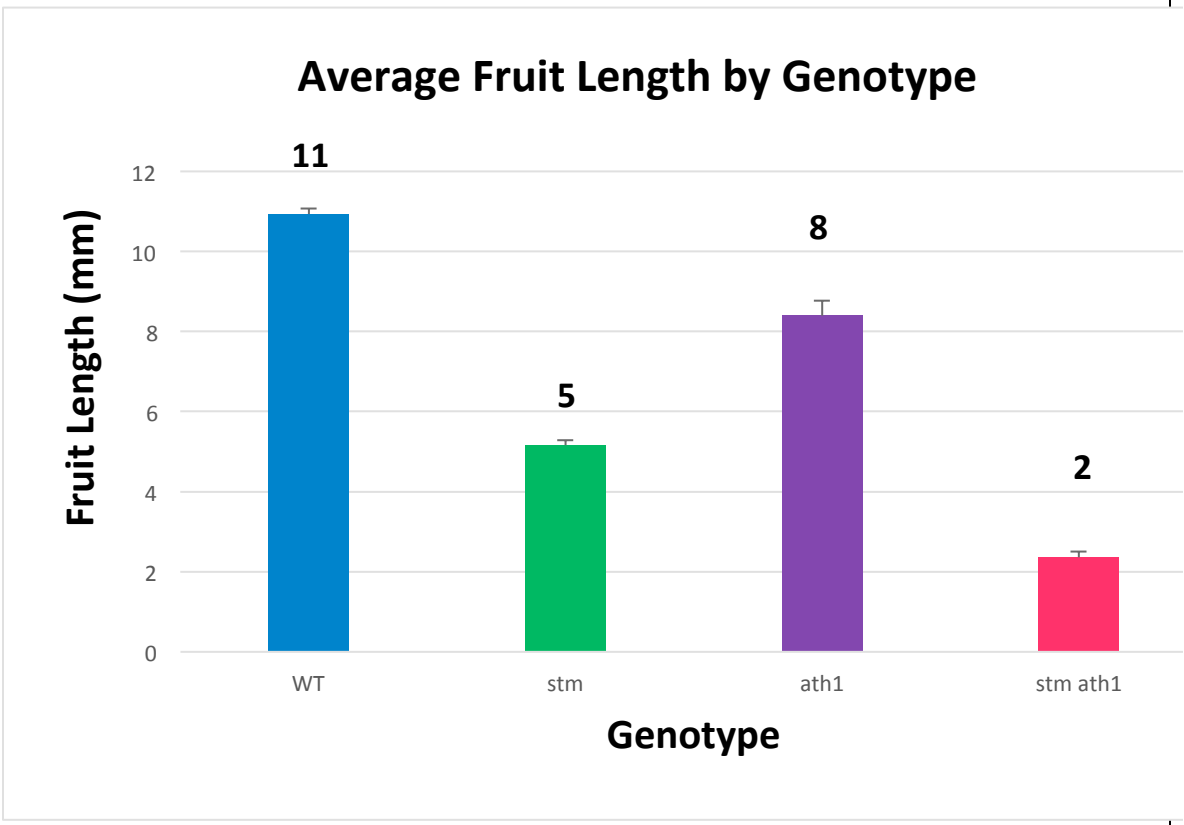

Figure 11: Average fruit length of wildtype, *stm, ath1,* and *stm/ath1* plants. n=50 for wildtype plants. n=232 for *stm* mutant plants. n=54 for *ath1* mutant plants. n=48 for *stm ath1* double mutant plants. The numbers above the bars denote the average fruit length for each genotype. Each of the mutants tested have significantly shorter fruit than wildtype. The *stm ath1* double mutants also have significantly shorter fruit than either of the single mutants. Of the eight *stm ath1* plants analyzed, seven produced one or more fruit that could be measured.

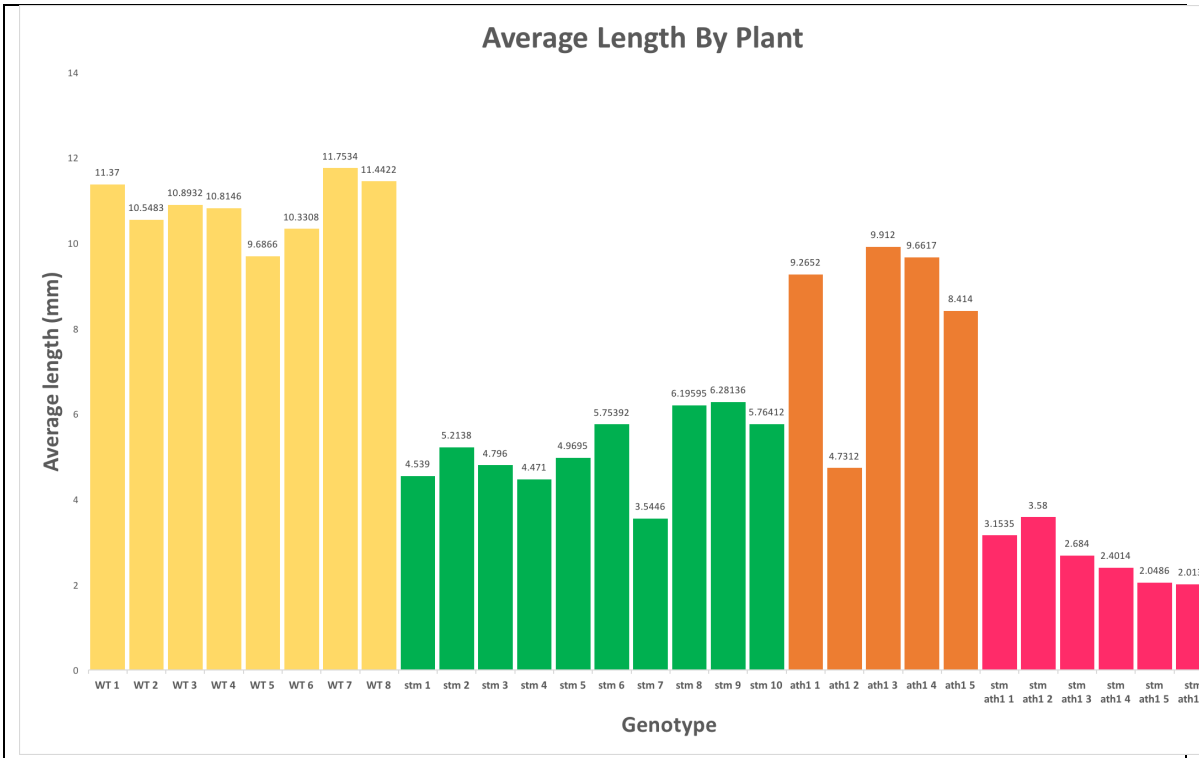

Figure 12: Average fruit length by plant. The average fruit length of each plant per genotype is shown. The average fruit length for each wild-type plant was about 11 mm. The average fruit length for each *stm* plant was about 5 mm with one outlier (*stm* 7*)*. The average fruit length for each *ath1* plant was about 9 mm with one outlier (*ath1* 2*)*. The average fruit length for each *stm ath1* plant was about 3 mm.

The average width of fruit for each genotype is shown in Table 6 and Figure 13. The *stm ath1* fruit structures produced were significantly narrower than those of either of the single mutants or of wildtype plants.

When examining the existing *stm ath1* fruit with a dissecting microscope to determine carpel number, it was notably more difficult to find the valve/replum

boundary. In many of the fruit with one or two carpels, this boundary was most distinct near the style.

Table 6: Average fruit width and standard deviations for wildtype, *stm, ath1,* and *stm ath1* plants.

Genotype	Average width (mm)	Standard deviation	Standard Error
WT	1.07	0.83	0.13
Stm	0.75	2.00	0.13
ath1	0.94	0.37	0.37
stm ath1	0.30	0.15	0.15

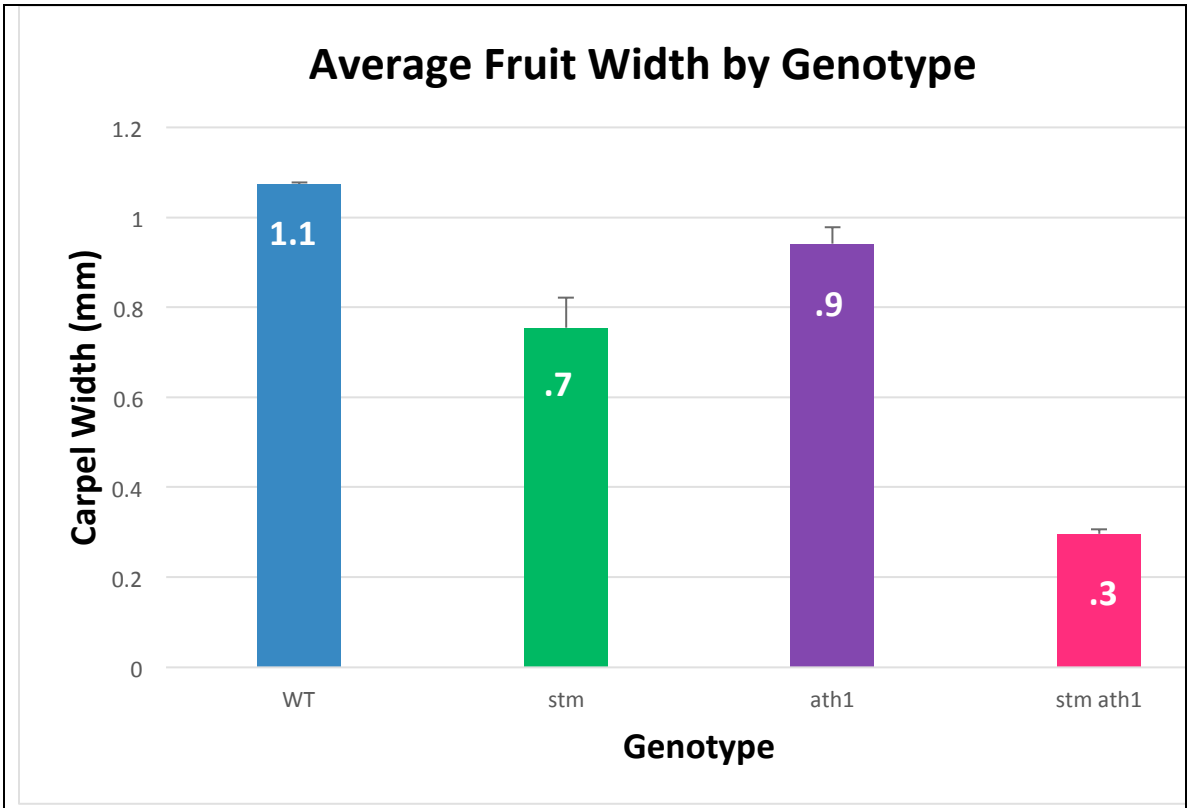

Figure 13: Average fruit width of wildtype, *stm, ath1,* and *stm ath1* plants. n=50 for wildtype plants. n=232 for *stm* mutant plants. n=54 for *ath1* mutant plants. n=48 for *stm ath1* double mutant plants. The numbers above the bars denote the average fruit width for each genotype. Compared to WT and each single mutant, *stm ath1* double mutants have a significant reduction in fruit width.

DISCUSSION

This project was designed to investigate the roles that *STM* and *ATH1* have in fruit development. My first hypothesis was that fruit size would be reduced in the *stm ath1* double mutant due to ATH1 and STM's role in flower meristem maintenance. I found that the majority of *stm ath1* flowers are missing a central pistil (Figure 9). Furthermore, by comparing the *stm ath1* fruit structures that were present to those of wild-type plants, I discovered that their average length (2.4 mm) and width (0.3 mm), were both significantly reduced compared to the average length (10.9 mm) and width (1.1 mm) of wild-type fruit (Figures 11 and 12). With partial loss of STM function, the *stm* fruit also had, on average, significantly reduced fruit length (5.2 mm) compared to wildtype fruit (Figure 11). The average length of *ath1* mutant fruit (8.4 mm) was also significant shorter than wild-type (Figure 11). These observations support my hypothesis that STM and ATH1 both regulate fruit size.

Since the STM transcription factor is essential for maintaining undifferentiated stem cells within the SAM and FM (Jasinki et al., 2005; Yanai et al., 2005), partial loss of STM function was expected to cause a reduction in the stem cell population available to make the fruit. Loss of ATH1 is also known to affect the size and organization of the vegetative SAM, but to a far less extent that loss of STM. *ath1* single mutants were found to have reduced number of meristematic cells and a decrease in diameter of SAM (Rutjens et al., 2009). My study revealed that disruption of ATH1 function substantially enhances the partial loss of STM function in the center of the floral meristem where the gynoecium is formed. While fruit with two carpels are consistently produced in both the *stm* and *ath1* single mutants, the majority of *stm ath1* flowers are missing a fruit entirely.

Since the carpels are the last organs produced by the FM (Girin et al., 2009), it is likely that the stem cell population in the majority of *stm ath1* flowers is not sufficient to produce a fruit. Even if some stem cells remain in *stm ath1* flowers to make a fruit, it is reduced in size. Overall, these results suggest that the loss of *STM* and *ATH1* gene function prevents the fruit from developing normally, which fits with previous observations that *stm ath1* plants are infertile (Liljegren, unpublished results).

A second hypothesis I tested was that the number of carpels in *stm ath1* fruit will be less than the two typically found in wildtype fruit. I predicted that if the *STM* and *ATH1* genes have overlapping roles in fruit development, there should be significant differences in carpel number in *stm ath1* double mutant plants compared to wildtype plants. I found that although carpel number was unaffected in either of the single mutants compared to wild-type (Figure 10), 90% of the *stm ath1* flowers examined either did not produce a fruit or produced fruit with less than two carpels (Figure 9). These results suggest that the presence of a functional ATH1 transcription factor is able to compensate for partial loss of STM in maintaining enough cells in the flower meristems to generate both carpels.

An open question that remains is whether possible defects in forming the valve/replum boundary contribute to the smaller fruit size and reduced carpel number of *stm ath1* double mutant fruit. Using a dissecting microscope, we observed that this boundary was more difficult to detect in *stm ath1* fruit with valve tissue than it was to find this boundary in single mutant fruit and wild-type fruit. This question can best be addressed by using scanning electron microscopy to allow for a clearer view of the valve-replum boundary in *stm ath1* fruit. The higher resolution of cells at the fruit surface

would show whether the valve margin boundaries are blurry compared to wild type, and could reveal what epidermal cell types remain in the *stm ath1* fruit without apparent valves (Figure 9). Examining hand sections of *stm ath1* fruit would also be useful to verify whether there are one or two seed chambers present. A *stm ath1* fruit that appeared to consist of a single carpel valve in my study could have been divided by an obscured valve margin boundary and/or show internal evidence of two seed chambers.

This work, in combination with other research projects, is providing a more complete picture of the phenotypic effects of mutations in the *STM* and *ATH1* genes. Palmer (2018) has found that these mutations prevent floral organ abscission. Malone (2018) has found that the total number of floral organs is reduced and that fusion between floral organs occurs. Roth (2018) and Leary (2018) have investigated whether mutations in an independent allele of *ATH1* are also able to uncover functional redundancy between ATH1 and STM in establishing the flower's organ boundaries. Of particular relevance to my study is an ongoing project on the fertility of *stm*, *ath1* and *stm ath1* fruit (Mason and Liljegren, unpublished results). Since my studies have revealed significant defects in the growth of *stm* and *stm ath1* fruit, he is performing an experiment to analyze the effects of mutation in *STM* and *ATH1* genes on seed production. The goal of this experiment is to investigate whether either of the single mutants or the *stm ath1* double mutant plants have reduced ovule and seed counts in comparison to wildtype and single mutants. In the future, ChIP-seq could be used to find where the STM and ATH1 transcription factors bind in the genome, which would open the door to pinpointing their immediate targets in producing floral organ boundary regions.

BIBLIOGRAPHY

Alonso-Cantabrana, H., Ripoll, J. J., Ochando, I., Vera, A., Ferrándiz, C. and Martínez-Laborda, A. (2007). Common regulatory networks in leaf and fruit patterning revealed by mutations in the *Arabidopsis ASYMMETRIC LEAVES1* gene. *Development* 134, 2663-2671.

Cole, M., Nolte, C. and Werr, W. (2006). Nuclear import of the transcription factor SHOOT MERISTEMLESS depends on heterodimerization with BLH proteins expressed in discrete sub-domains of the shoot apical meristem of *Arabidopsis thaliana*. *Nucleic Acids Res.* 34, 1281-1292.

Dinneny, J. R., Weigel, D. and Yanofsky, M. F. (2005). A genetic framework for fruit patterning in *Arabidopsis thaliana*. *Development* 132, 4687-4696.

Endrizzi, K., Moussian, B., Haecker, A., Levin, J. Z. and Laux, T. (1996). The *SHOOT MERISTEMLESS* gene is required for maintenance of undifferentiated cells in *Arabidopsis* shoot and floral meristems and acts at a different regulatory level than the meristem genes *WUSCHEL* and *ZWILLE*. *Plant J.* 10, 967-979.

Ferrándiz, C., Liljegren, S. J. and Yanofsky, M. F. (2000). Negative regulation of the *SHATTERPROOF* genes by FRUITFULL during *Arabidopsis* fruit development. *Science* 289, 436-438.

Girin, T., Sorefan, K. and Østergaard, L. (2009). Meristematic sculpting in fruit development. *J Exp Bot.* 60, 1493–1502.

Gomez-Mena, C. and Sablowski, R. (2008). *ARABIDOPSIS THALIANA HOMEOBOX GENE1* establishes the basal boundaries of shoot organs and controls stem growth. *Plant Cell* 20, 2059–2072.

Gu, Q., Ferrándiz, C., Yanofsky, M. F. and Martienssen, R. (1998). The *FRUITFULL* MADS-box gene mediates cell differentiation during *Arabidopsis* fruit development. *Development* 125, 1509-1517.

Hepworth, S. R. and Pautot, V. A. (2015). Beyond the divide: boundaries for patterning and stem cell regulation in plants. *Front Plant Sci* 6, 1052, 1-19.

Jasinski, S., Piazza, P., Craft, J., Hay, A., Woolley, L., Rieu, I., Phillips, A., Hedden, P. and Tsiantis, M. (2005). KNOX action in *Arabidopsis* is mediated by coordinate regulation of cytokinin and gibberellin activities. *Current Biology* 15, 1560-1565.

Leary, L. (2018). Characterizing the effects of *stm* and *ath1* mutations on floral organ development in *Arabidopsis thaliana.* Undergraduate honors thesis, Department of Biology, University of Mississippi.

Liljegren, S. J., Ditta, G. S., Eshed, Y., Savidge, B., Bowman, J. L. and Yanofsky, M. F. (2000). *SHATTERPROOF* MADS-box genes control seed dispersal in *Arabidopsis*. *Nature* 404, 766-770.

Liljegren, S. J., Roeder, A. H., Kempin, S. A., Gremski, K., Ostergaard, L., Guimil, S., Reyes, D. K. and Yanofsky, M. F. (2004). Control of fruit patterning in *Arabidopsis* by INDEHISCENT. *Cell* 116, 843-853.

Long, J. A., Moan, E. I., Medford, J. I. and Barton, M. K. (1996). A member of the KNOTTED class of homeodomain proteins encoded by the *STM* gene of *Arabidopsis*. *Nature* 379, 66–69.

Malone, H. (2018). Characterizing the effects of mutations in *STM* and *ATH1* on floral organ development in *Arabidopsis thaliana.* Undergraduate honors thesis, Department of Biology, University of Mississippi.

Meinke, D. W., Cherry, J. M., Dean C., Rounsley S. D. and Koornneef M. (1998). *Arabidopsis thaliana*: A model plant for genome analysis. *Science* 282, 662–682.

Müller, A. (1961). Zur Charakterisierung der Blüten und Infloreszenzen von *Arabidopsis thaliana* (L.) Heynh. *Kulturpflanze* 9, 364-393.

Palmer, S. (2018). Quantifying abscission defects in mutant *Arabidopsis thaliana* flowers. Undergraduate honors thesis, Department of Biology, University of Mississippi.

Penin, A. A. and Logacheva, M. D. (2011). Correlation between number and position of floral organs in *Arabidopsis*. *Ann. Bot*. 108, 123–131.

Quaedvlieg, N, Dockx, J., Rook, F., Weisbeek, P. and Smeekens, S. (1995). The homeobox gene *ATH1* of *Arabidopsis* is derepressed in the photomorphogenic mutants *cop1* and *det1*. *Plant Cell* 7, 117–129.

Ripoll, J. J., Roeder, A. H. K., Ditta, G. S. and Yanofsky, M. F. (2011). A novel role for the floral homeotic gene *APETALA2* during *Arabidopsis* fruit development. *Development* 138, 5167-5176.

Roeder, A. H., Ferrandiz, C. and Yanofsky, M. F. (2003). The role of the REPLUMLESS homeodomain protein in patterning the *Arabidopsis* fruit. *Curr. Biol.* 13, 1630-1635.

Roth, H. (2018). The effects of mutations in the *ATH1* and *STM* genes on sepal, petal, and stamen abscission in *Arabidopsis thaliana* plants. Undergraduate honors thesis, Department of Biology, University of Mississippi.

Rutjens, B., Bao, D., van Eck-Stouten, E., Brand, M., Smeekens, S. and Proveniers, M. (2009). Shoot apical meristem function in Arabidopsis requires the combined activities of three BEL1-like homeodomain proteins. *Plant J.* 58, 641-654.

Scofield, S., Dewitte, W. and Murray, J.A. (2014). STM sustains stem cell function in the Arabidopsis shoot apical meristem and controls KNOX gene expression independently of the transcriptional repressor AS1. *Plant Signal Behav.* 9, e28934.

Smyth, D. R., Bowman, J. L. and Meyerowitz, E. M. (1990). Early flower development in *Arabidopsis*. *Plant Cell* 2, 755–767.

Yanai, O., Shani, E., Dolezal, K., Tarkows, P., Sablowski, R., Sandberg, G., Samach, A. and Ori, N. (2005). *Arabidopsis* KNOXI proteins activate cytokinin biosynthesis. *Curr. Biol.* 15, 1566–1571.